INDIAN JOURNAL OF SCIENCE AND TECHNOLOGY

RESEARCH ARTICLE

Analytic Influence of Thermally Radiation and Buoyancy Flow Model Under the Impact of Higher Order Chemical Reaction, with Suspension of Micro-organism

Boreddy Mahendar Reddy[1], P Sreehari[1], Rama Udai Kumar[2], S Jagadha[3], D Gopal[4]*, N Kishan[1]

1 Department of Mathematics, UCS, Osmania University, Hyderabad, 500007, Telangana, India
2 Department of Mathematics, Pallavi Engineering College, Kuntloor, Hyderabad, 501505, Telangana, India
3 Department of Mathematics, Institute of Aeronautical Engineering, Dundigal, Hyderabad, 500043, Telangana, India
4 Junior Lecturer in Mathematics, Telangana Tribal Welfare Upgraded Residential Junior College for Boys, Cheemanpally, Nizamabad, 503165, Telangana, India

OPEN ACCESS

Received: 25-09-2024
Accepted: 22-10-2024
Published: 29-11-2024

Citation: Reddy BM, Sreehari P, Kumar RU, Jagadha S, Gopal D, Kishan N (2024) Analytic Influence of Thermally Radiation and Buoyancy Flow Model Under the Impact of Higher Order Chemical Reaction, with Suspension of Micro-organism. Indian Journal of Science and Technology 17(43): 4558-4570. https://doi.org/10.17485/IJST/v17i43.3075

* **Corresponding author**.

degavath.gopal@gmail.com

Funding: None

Competing Interests: None

Published By Indian Society for Education and Environment (iSee)

ISSN
Print: 0974-6846
Electronic: 0974-5645

Abstract

Objective: This study is centered on the numerical investigation of bio-convection has granted significant application in the engineering and manufacturing of advanced aircraft, cosmetic production, enhanced defense types of equipment, medicines, and treatment of various diseases and batteries. The phenomenon of the buoyancy flow model, the impact of thermal radiation with a suspension of micro-organisms is demonstrated around a cone and paraboloid. Here, the flow is studied with the effect of higher-order chemical reactions with micro-organisms. **Methods:** Initially, physical systems were demonstrated as non-linear partial differential equations. Through, appropriate transformations, numerically tackled the transformed ODE's by employing the Bvp4c scheme. The relevant flow parameters of salient features are illustrated over numerical outcomes and employing the R-K numerical method physical interpretations are explained graphically. **Outputs:** The results reveal chemical reaction parameter decrement velocity and temperature profile and increment in concentration. Here, graphical representation elucidated various physical attributes of the system. The performance of dimensionless quantifiers is examined clearly. **Novelty:** As labeled in the results, heterogeneous is the examination of thermal radiation in science and technology such as liquid metal fluids different momentum devices for missiles, and turbines of gas effects on thermal radiation are exhibited and distinguished in various investigations and numerous applications due to radiative emission in the energy distribution for higher inputs which are illustrated in the existing literature. The innovative physical significance of thermally radiation and buoyancy flow

model with suspension of micro-organism strength and described on non-dimensional parameters. The innovative physical significance of thermally radiation and buoyancy flow model with suspension of micro-organism strength and described on non-dimensional parameters.

Keywords: Thermal radiation; Buoyancy flow; Chemical reaction; Heat and mass transfer; Subtle body of revolution

1 Introduction

Nowadays, dynamics of non-Newtonian dimensionless governing flow have extensive applications and have gained the dominant role in the fields of drive engineering, , agriculture, building power plants, and mining. The demand for physiological liquids, dental creams, cleansers, construction, and salt arrangements is playing a crucial position and its demand is increasing due to the properties of non-Newtonian fluids. The essential nonlinear property of connectivity between shear force and rate of shear strain. Saleem et al.[(1)] have a great number of works focused on bio-convection issues and exploring suspensions comprising solid particles in different facets of research issues. Aaqib et al.[(2)] explore MHD motile gyrostatic micro-organisms flow comprising tiny nanoparticles on the analysis of thermal radiation towards a nonlinear surface with velocity slip. Yang et al.[(3)] delved into exploring the migration of buoyancy forced by the fluid particles of laminar governing flow as well as in water resources. The solution is given for the concentration distribution of buoyancy-controlled particles and the effects of peclet number on the dispersion of active particles are given. Majeed et al.[(4)] performed Non-newtonian MHD fluid flow into the occurrence of thermal radiation over the stretchable porous surface with the effect of 3D chemically reactive.

The theory of bio-convection fluid flow has gained much attention in the past years due to a novel division of biological and industrial fluid mechanics in which bio-convection has encouraged fluid flow by the macroscopic convective waves because of the interruption of enhanced spinning mobile microorganisms (denser than the medium). At having upper surface of the fluid, the self-driven suspended microorganisms are agglomerated due to unbalanced density stratification causing the existence of bio-convection spirals. In bio-convection a small-sized microbe floats enter into the enhanced parts of a fluid flow, producing asymmetrical establishment and uncertainty. The gyrotactic micro-organisms which is algae near to accrue in the greater layer of fluid which sources an unbalanced highest consequential of substantial density maintenance due to rapid swimming. Maheshet al.[(5)] developed a continuum model for the bio-convection. Kumar et al.[(6)] studied the suspension of mixed bio-convection in hydro-magnetic unsteady slip stagnation flow of nano-fluid. Sangeethaet al.[(7)] deliberated an expression of bio-convection that has pronounced hydrodynamic unpredictability and outlines in life-swimming body fluids.

In heterogeneous areas, the examination of thermal radiation in manufacturing has liquid metal fluids varied momentum strategies for missiles, gas turbines, and fourth advances nuclear power plants, surface heat transfer is exhibited very small coefficient of convective heat transfer. All aforementioned studies and numerous investigations are distinguished thermal radiation due to the perception that glowing emission depends on temperature. Several[(8,9)] investigators have delved into exploring thermal radiation in different facets. The researchers Ellahi[(10)] and Mehboob et al.[(11)] discussed the impacts of MHD and Newtonian nanofluid flow in a pipe as well as the analytic investigation of thermal radiation. Zeeshan et al.[(12,13)] analyzed Jeffrey nanofluid via an exponential stretching sheet and optimized entropy generation. Khan et al.[(14)] investigated heat transformation in Darcy flow with conectaining gyrotactic microorganisms. Recently researchers[(15–19)] discussed the numerical simulation of

bioconvective gyrotactic microorganisms.

The main aim of this exploration is to analyze the chemical reaction on the buoyancy-driven flow of thermal radiation with the suspension of micro-organisms; which are all applied to the flow of parabolic and cone of revolution to establish governing equations. The innovative physical significance of thermally radiation and buoyancy flow model with suspension of micro-organism strength and described on non-dimensional parameters. Wave vacillations in the thermal edge sheet of nano-fluid movement below solar radio activity section along a buoyancy-driven porous plate. Sangeetha et al.[20] illustrated biological-based magneto nanoparticles motion, microorganisms of Maxwell as well as Casson nano-liquid transversely the Darcy and non-Darcy permeable surfaces with the impact of buoyancy, Hall, solar energy, heat dissipation, activation energy, Ohmic temperature.

2 Mathematical Formulation

Researchers, scrutinized thermal radiation and chemical reaction, infusion-induced revolution position around slender bodies with buoyancy effects of transportation phenomena. From Figure 1, the graphical revealed that the energy distribution of the uniform uniform at T_w, the unvarying exceeding temperature value T_∞ is observed from the surface far away and the flow's structure. The cylindrical system represents in (x,r), the vertex of the body located at the origin. The concentration of the surface is taken uniformly $C_w$whereas the relevant ambient fluid is considered as C_∞. The coordinate denotes the equilibrium distance between distinct forms of slender revolutions and rotating slender surfaces in a vertical position. In this nanofluid flow line segment, higher non-linearly ordinary differential equations and boundary conditions are formulated and computed[21,22] and the governing equations describing phenomena incorporating Boussinesq approximations, Darcy saturated porous media, thermophoretic effects, Brownian motion, and properties of thermal radiation are detailed.

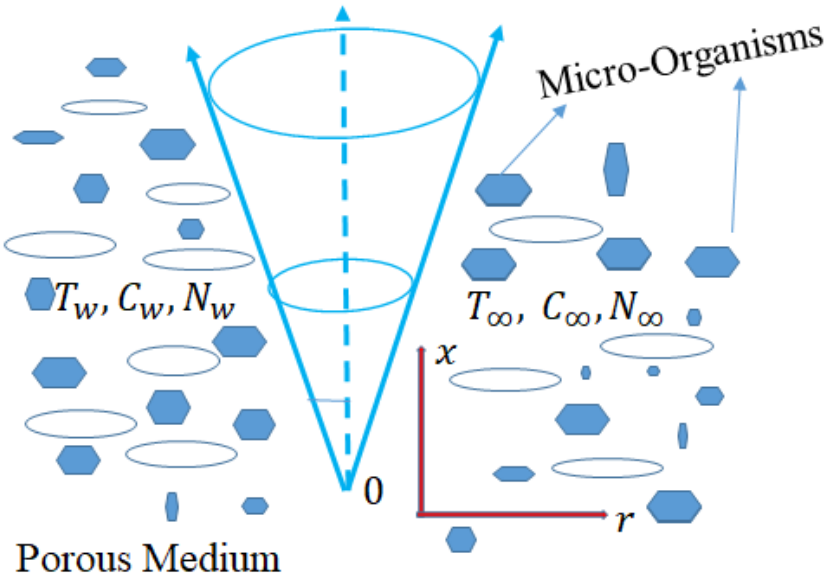

Fig 1. Geometrical flow model

$$\frac{\partial (ru)}{\partial x} + \frac{\partial (rv)}{\partial r} = 0 \tag{1}$$

$$\frac{1}{r}\frac{\partial \psi}{\partial r} = \left(\frac{Kg}{\upsilon}\right)((T - T_\infty)\beta_T + (C - C_\infty)\beta_C) \tag{2}$$

$$\frac{\partial T}{\partial x}\frac{\partial \psi}{\partial r} - \frac{\partial T}{\partial r}\frac{\partial \psi}{\partial x} = \alpha\frac{\partial}{\partial r}\left(r\frac{\partial T}{\partial r}\right) + \frac{\partial q_r}{\partial z} + (r\tau)\left(\frac{D_T}{T_\infty}\left(\frac{\partial T}{\partial r}\right)^2 + D_B\frac{\partial T}{\partial r}\frac{\partial C}{\partial r}\right) \tag{3}$$

$$\frac{\partial C}{\partial x}\frac{\partial \psi}{\partial r}-\frac{\partial C}{\partial r}\frac{\partial \psi}{\partial x}=D_B\frac{\partial}{\partial r}\left(r\frac{\partial C}{\partial r}\right)+\left(\frac{D_T}{T_\infty}\right)\frac{\partial}{\partial r}\left(r\frac{\partial T}{\partial r}\right)-K^*(C-C_\infty)^n \tag{4}$$

$$\frac{\partial N}{\partial x}\frac{\partial \psi}{\partial r}-\frac{\partial N}{\partial r}\frac{\partial \psi}{\partial x}+\frac{bw_c}{C_\infty}\left(\frac{\partial}{\partial r}\left(N\frac{\partial C}{\partial r}\right)\right)=D_n\frac{\partial}{\partial r}\left(r\frac{\partial N}{\partial r}\right) \tag{5}$$

Where assumed Boussinesq estimate is

$$\left(\frac{\rho}{\rho_\infty}\right)=(-1)\left[-1+\beta_T(T-T_\infty)+\beta_C(C-C_\infty)\right] \tag{6}$$

With the subjected boundary conditions being:

At, $r=R(x)$

$$v=0, T=T_w(x)-T_\infty=Ax^{(a)}, C=C_w(x)-C_\infty=Bx^{(b)}, N=N_w(x)=Nx^{(c)} \tag{7}$$

$u=0, T=T_\infty, C=C_\infty, N=N_\infty Atr\to\infty$

Rosseland approximation can be written for thermal radiation

$$q_r=-\frac{4\gamma^*}{3k^*}.\frac{\partial T^4}{\partial r} \tag{8}$$

Expressed T^4employing a Taylor series as a linear function of the distributed temperature T_∞.

$$T^{(4)}=4TT_\infty^{(3)}-3T_\infty^{(4)} \tag{9}$$

Substituting Equation (9) in Equation (8), Equation (3) reduced to

$$\frac{\partial T}{\partial x}\frac{\partial \psi}{\partial r}-\frac{\partial T}{\partial r}\frac{\partial \psi}{\partial x}=\alpha\left(1+\frac{4}{3}Nr\right).\frac{\partial}{\partial r}\left(r\frac{\partial T}{\partial r}\right)+r\tau\left(\frac{D_T}{T_\infty}\left(\frac{\partial T}{\partial r}\right)^2+D_B\frac{\partial T}{\partial r}\frac{\partial C}{\partial r}\right)$$

Here $Nr=\frac{4\gamma^*T_\infty^{(3)}}{kk^*}$is defined as thermal radiation.

The dimensionless expression of functions by utilizing similarity variables are $f(\eta),\theta(\eta),\phi(\eta)$ and $\chi(\eta)$are defined as

$$\begin{gathered}\eta=Ra\left(\frac{r}{x}\right)^2, Ra=\frac{Kg\beta_T(T_w-T_\infty)x}{\alpha v}, u=\left(\frac{1}{r}\right)\frac{\partial \psi}{\partial r}, v=\left(-\frac{1}{r}\right)\frac{\partial \psi}{\partial r}, \psi=(\alpha x)f(\eta),\\ T-T_\infty=\theta(\eta)(T_w-T_\infty), C-C_\infty=\phi(\eta)(C_w-C_\infty), N-N_\infty=\chi(\eta)(N_w-N_\infty)\end{gathered} \tag{11}$$

where ψ(stream function), Ra (modified local Rayleigh number)

Because of $\eta=\eta_0$(η_0 is indicated as the fixed constant) and represents mathematically a revolution of the body's minor value, It is considering the shape of the slender revolution and size of the slender revolution. The Equation (11) is listed below:

$$R(x)=\left(\frac{v\alpha\eta_0}{Kg\beta_TA}\right)^{1/2}x^{\left(\frac{1-a}{2}\right)}$$

It is visualized that, in real-world relevance the parameter a must adhere to $a\leq 1$. For instance, corresponding to $a=-1$recalcitrant resulting in a cone shape, corresponding to $a=0$ revolution resulting in paraboloid.

The reduced governing equations are as follows:

$$f'(\eta)=\frac{1}{2}\left(\theta(\eta)+Nc\phi(\eta)\right) \tag{12}$$

$$\left(1+\frac{4}{3}Nr\right)\theta''(\eta)=\frac{1}{2}\eta\left(af'(\eta)\theta(\eta)-f(\eta)\theta'(\eta)-2\theta'(\eta)\right)\left(Nb\theta'(\eta)\phi'(\eta)+Nt\theta'(\eta)^2\right) \tag{13}$$

$$\phi^{''}(\eta)=\frac{1}{2}\eta\left(bLef^{'}(\eta)\phi(\eta)-Lef(\eta)\phi^{'}(\eta)-2\phi^{'}(\eta)-\frac{2}{Le}\left(\frac{Nt}{Nb}\right)\left(\theta^{'}(\eta)+\theta^{''}(\eta)\right)-\gamma\phi^{n}\right) \tag{14}$$

$$\chi^{''}(\eta)=\frac{1}{2}\eta\left(cLef^{'}(\eta)\chi(\eta)-Lef(\eta)\chi^{'}(\eta)+pe\begin{pmatrix}\chi(\eta)\phi'(\eta)+2\phi\chi'\eta\\+2\eta\chi(\eta)\phi''(\eta)\end{pmatrix}-2\chi^{'}(\eta)\right) \tag{15}$$

The associated boundary conditions of governing equations are:

$$\eta=\eta_0, f(\eta)+(a_1-1)\eta f^{'}(\eta)=0, \theta(\eta)=1, \phi(\eta)=1, \chi(\eta)=1$$

$$\eta\to\infty, f^{'}(\eta)=0, \theta(\eta)=0, \phi(0)=0, \chi(\eta)=0$$

Here, $Nc=\frac{\beta_{c1}(C_w-C_\infty)}{\beta_{T1}(T_w-T_\infty)}$ the ratio of buoyancy, $Nb=\frac{D_B\tau(C_w-C_\infty)}{\alpha}$ (Brownian parameter), $Nt=\frac{D_T\tau(T_w-T_\infty)}{T_\infty\alpha}$ thermophoresis constant, $Le=\frac{\alpha}{D_B}$ lewis number, $pe=\frac{bw_c}{D_n}$ Peclet number.

This study's Equations Equations (12), (13), (14) and (15) facilitate two distinct numerical solutions:

- If the value of a and b is zero, then the governing flow revolution is a paraboloid.
- If the value of a = 1and b=-1, then the governing flow revolution is a paraboloid.

The physical quantities of interest are constants in the real-world connectivity of thermal and mass diffusion, they are defined as follows.

$$Nu=\frac{hy}{k}=-\left(\left|\frac{\partial T}{\partial r}\right|_{r=R(x)}\right)/(T_w-T_\infty)=-2\eta_0^{0.5}Ra^{0.5}\theta^{'}(\eta_0)$$

$$Sh=\frac{mx}{D_B(C_w-C_\infty)}=-2\eta_0^{0.5}Ra^{0.5}\phi^{'}(\eta_0)$$

$$NSh=\frac{mx}{D_B(N_w-N_\infty)}=-2\eta_0^{0.5}Ra^{0.5}\chi^{'}(\eta_0).$$

3 Numerical Scheme

In this nanofluid flow line segment, higher non-linearly ordinary differential equations and boundary conditions are formulated and computed by Bvp4c via MATLAB. As the governing flow control equations possess many independent variables, they are presented in partial derivatives. The partial derivatives are converted into ordinary differential equations. The transformation of differential equations into a first-order system is executed by similarity variable. First-order differential equations system $y^{'}=f(x,y)$ are integrated in the interval range of $[a,b]$, substance to the flow circumstances of the system prescribed as $(y(a),y(b))=0$. The numerical method Runge-Kutta fourth-order is employed to solve non-linear ordinary differential equations. A set of non-linear ordinary differential equations is obtained in the form of second-order f,θ and ϕ. The reduction of the above non-linear differential equations leads to simultaneous equations. Moreover, the values of $f^{'},\theta,\phi$ are presented when $\eta\to\infty$with the aid of these boundary end conditions, the unknown initial conditions at $\eta\to 0$using shooting technique. In the shooting method, the boundary value problems are reduced into to an initial value problem by assuming initial values. The calculation of boundary value should match with the real boundary value as possible. The most important step is to select the appropriate finite value of boundary condition far field. We presented infinity condition at a large but finite value of η, there is no variation in velocity, temperature, and concentration. We computed a maximum value of η=6 which is sufficient to get the target of far-field boundary conditions asymptotically for all values of nondimensional parameters are taken.

Association polynomial offers a fourth-order accuracy of continuous governing flow explanation via range interval [a, b] with this formula. Considered 10^{-6}convergence criteria.

$$f(\eta)=y(1)$$

$$f^{'}(\eta) = y(2)$$

$$f^{''}(\eta) = y(3)$$

$$y(2) = \frac{1}{2}(y(4) + Ncy(7))$$

$$\theta(\eta) = y(4), \theta^{'}(\eta) = y(5), \theta^{''}(\eta) = y(6), \phi(\eta) = y(7), \phi^{'}(\eta) = y(8), \phi^{''}(\eta) = y(9),$$

$$\left(1 + \frac{4}{3}\right) Nry(6) = \frac{1}{2}\eta(ay(2)y(4) - y(1)y(5) - 2y(5)) - (Nby(5)y(8) + Nty^2(5))$$

$$y(9) = \frac{1}{2}\eta\left(bLey(2)y(4) - Ley(1)y(8) - 2y(5) - \frac{2}{Le}\left(\frac{Nt}{Nb}\right)(y(5) + y(6 - \gamma y^n(1)))\right)$$

$$\chi(\eta) = y(10), \chi^{'}(\eta) = y(11), \chi^{'}(\eta) = y(12)$$

$$y(12) = \frac{1}{2}\eta\left(cLey(2)y(10) - Ley(1)y(11) + pe\begin{pmatrix} y(10)y(5) + \\ 2y(7)y(11)n + 2ny(10)y(9) \end{pmatrix} - 2y(11)\right)$$

Corresponding edge circumstances having

$$y_a(1) + (A-1)Ny_a(2) = 0, y_a(4) = 1, y_a(10) = 1$$

$$y_b(2) = 0, y_b(4) = 0, y_b(10) = 0$$

Geometric scaling and the development of dynamic simulation-based research are evaluated by employing nondimensional parameters. This paper uses thermophoresis, Brownian parameters, radiation, Peclet, and chemical reactions.

From the above non-dimensional parameters are the illustrations of the physical consequence of the buoyancy flow model with micro-organism governing flow, and the flow control outputs of the internal flow region are demonstrated graphically employing MATLAB Software using with shooting technique.

4 Results and discussion

Physical systems were demonstrated as non-linear partial differential equations. The relevant flow parameters of salient features are illustrated over numerical outcomes and by employing the R-K numerical method physical interpretations are explained. To contemporary the influences of all geometrical physical parameters of non-dimensional quantifiers of values are fixings Chemical reaction parameter $(n = 1)$, thermophoresis parameter$(Nt = 0.2)$, Brownian parameter $(Nb = 0.5)$, Peclet number $(Pe = 2.0)$, thermal radiation $(Nr = 1.0)$on the velocity gradient $(f^{'}(\eta))$, energy field $(\theta(\eta))$, concentration $(\phi(\eta))$, and motile micro-organism profiles $(\chi(\eta))$. The numerical R-K scheme is coded using MATLAB in the above micro-organism suspended flow segment and illustrated numerical results through graphs against various relevant nondimensional parameters. The graphs are displayed in the physical interpretations from Figures 2, 3, 4, 5, 6, 7, 8, 9, 10, 11, 12 and 13.

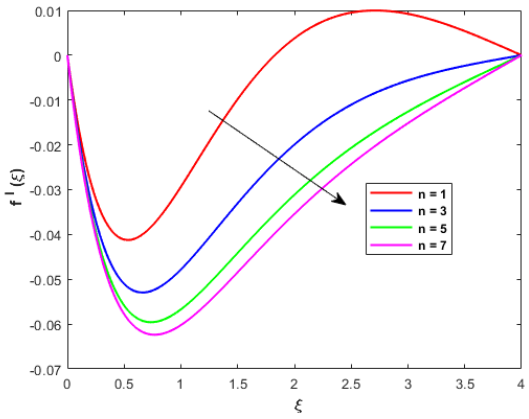

Fig 2. The behavior of the Chemical reaction parameter (n=1,3,5,7) on $f'(\xi), \theta(\xi)$

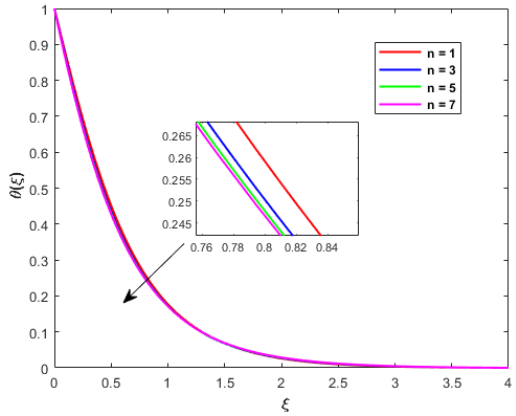

Fig 3. The behavior of the Chemical reaction parameter (n=1,3,5,7) on $f'(\xi), \theta(\xi)$

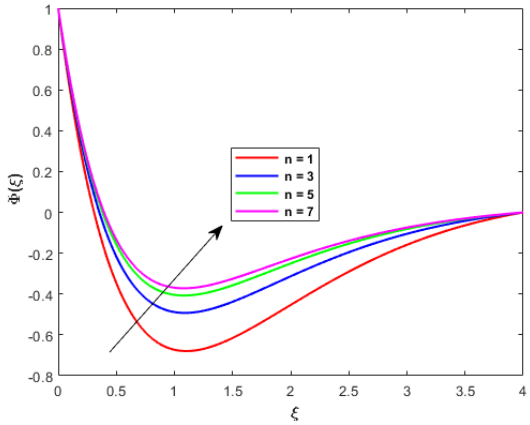

Fig 4. The behavior of Chemical reaction parameter (n=1,3,5,7) on $\phi(\xi), \chi(\xi)$

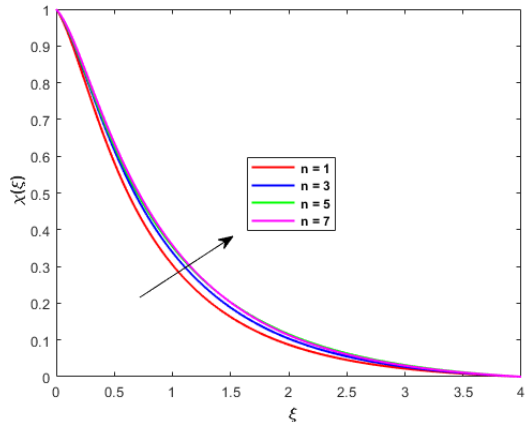

Fig 5. The behavior of Chemical reaction parameter r (n=1,3,5,7) on $\phi(\xi), \chi(\xi)$

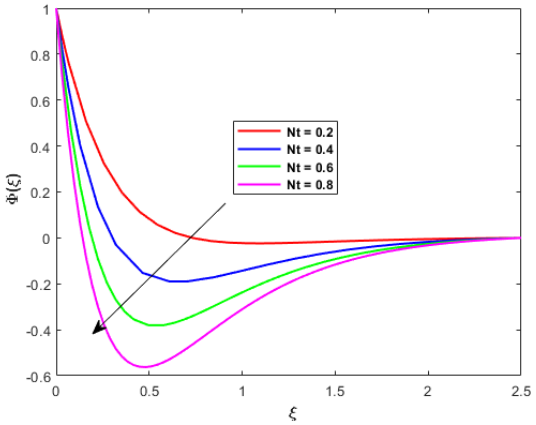

Fig 6. The behavior of thermophoresis parameter (Nt=0.2,0.4,0.6,0.8) on $\phi(\xi), \chi(\xi)$

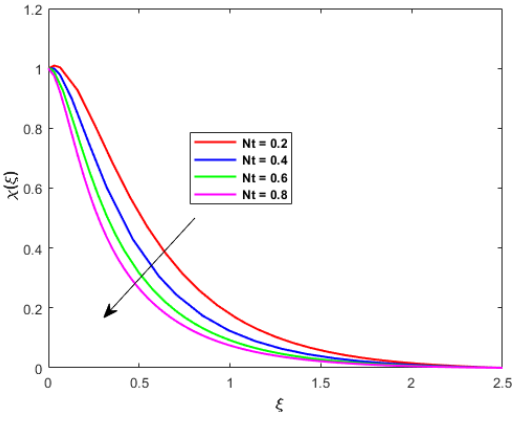

Fig 7. The behavior of thermophoresis parameter (Nt=0.2,0.4,0.6,0.8) on $\phi(\xi), \chi(\xi)$

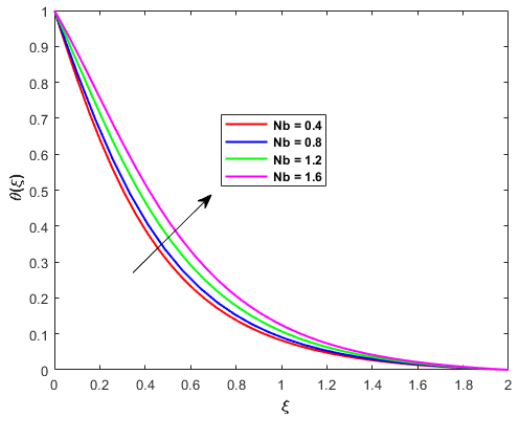

Fig 8. Behavior of Brownian motion parameter (Nb=0.4,0.8,1.2,1.6) on $\theta(\xi),\ \phi(\xi)$

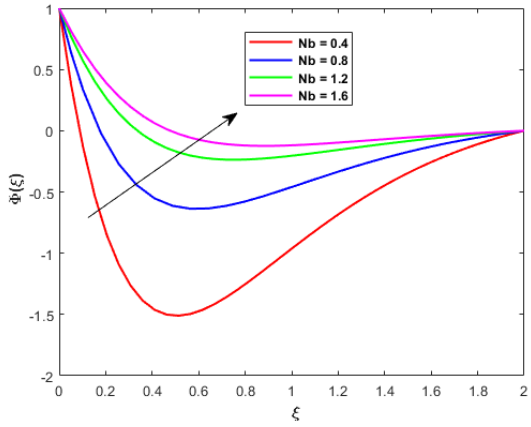

Fig 9. Behavior of Brownian motion parameter (Nb=0.4,0.8,1.2,1.6) on$\theta(\xi),\ \phi(\xi)$

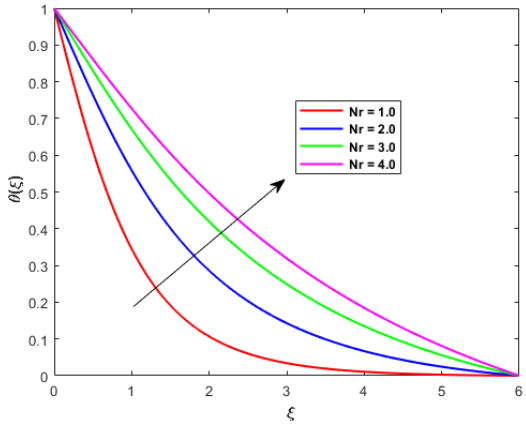

Fig 10. The behavior of Thermal radiation (Nr=1.0, 2.0, 3.0,4.0) on $\theta(\xi),\ \chi(\xi)$

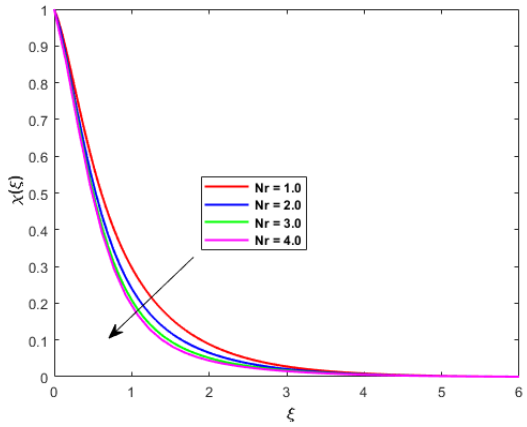

Fig 11. The behavior of Thermal radiation (Nr=1.0, 2.0, 3.0,4.0) on $\theta(\xi),\ \chi(\xi)$

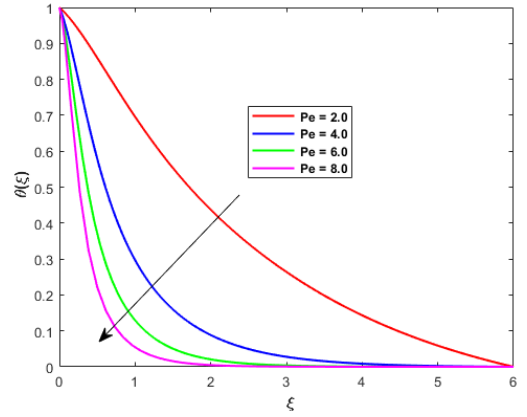

Fig 12. The behavior of Peclet number (Pe=2,4,6,8) on $\theta(\xi),\ \chi(\xi)$

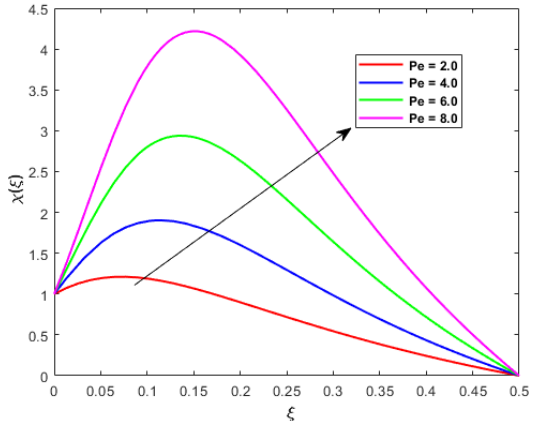

Fig 13. The behavior of Peclet number (Pe=2,4,6,8) on $\theta(\xi),\ \chi(\xi)$

From Figure 2 and Figure 3 observed that the enhancement of chemical reaction parameters $(n = 1,3,5,7)$ depreciated both velocity coefficient and temperature profiles. The chemical reaction procedure is that involves the movement of the ionic construction of a substance or molecular, its various forms changing physically from or nuclear reaction. The velocity outline and temperature simultaneously demonstrate a decline. The mechanism behind the inspiration of the outcome of chemical reaction frequency on the velocity outlines is connected with the interaction between chemical reaction and fluid flow. Figure 4 and Figure 5 depict the chemical reaction rate increases, increase in concentration, and micro-organism profile. Figure 6 and Figure 7 by increasing the values of the thermophoresis parameter $(Nt = 0.2,0.4,0.6,0.8)$, resulting in a depletion of concentration and micro-organisms outstanding to intensified thermophoresis diffusivity. Generally, Figure 8 and Figure 9 Brownian motion at the boundary layer supports heating the fluid and instantly diminishes particle testimony away from the fluid on the surface. Increment Nb intensifies particle collision, producing additional heat. Therefore, the increment of Brownian motion Nb shows ascent in concentration and temperature. Figure 10 and Figure 11 depicts higher thermal radiation parameter Nr shows depletion in micro-organisms and increasing in temperature fields. Figure 12 and Figure 13, as Peclet number $(Pe = 2,4,6,8)$ increases, the temperature field diminishes and shows an ascent in micro-organisms.

Table 1 shows that the current literature has compared the convergent [16–18] values of skin friction coefficient has a different case for our current study as compared with existing numerical values. Table 2 describes about Nusselt number and Sherwood number for numerous values of all relevant constraints. From a table Nusselt number $(Nu)$and Sherwood number (Sh)results are deliberated with the influence of enriching radiation parameter $(Nr = 0.5,1.0,1.5)$ on Nusselt number (Nu) has enhanced the Sherwood number (Sh) has enhanced the numerical results. Impact of enhancing Brownian parameter $(Nb = 0.1,0.3,0.5)$ on Nusselt number (Nu) has enhanced and also in Sherwood number (Sh) has declined numerically. From Brownian motion, parameter has an inverse proposition reaction that exists in the thermal radiation parameter. With the impact of enhanced Peclet parameter $(Pe = 1.2,1.4,1.6)$ on Nusselt number (Nu) has increased numerically and Sherwood's number has enhanced in both. Impacts of enhanced Levise number $(Le = 0.3,0.6,0.9)$ on Nusselt number (Nu) has enhanced numerically and in Sherwood number has been enhanced. The current study can also be diminished to micro- organisms of nano-fluid exhausting $Nr = 0$.

Table 1. Numerical comparison table of Skin friction coefficient

A	Present results	Bhatti [23]	Mustafa [24]	Ibrahim [25]
0.1	-0.96941	-0.9694	-0.9694	-0.9694
0.5	-0.66730	-0.6673	-0.6673	-0.6673
1.0	0.00000	0.0000		
2.0	2.01751	2.0175	2.0175	2.0175

Table 2. Mathematical values of Nussult number

Nr	Nb	Nt	Pe	a1	Le	Nu=Ra$^{0.5}\theta'(\eta_0)$	Sh=Ra$^{0.5}\phi'(\eta_0)$
0.5	0.1	0.5	1.2	0.2	0.3	0.310381	0.458781
1.0						0.423819	0.581700
1.5						0.499953	0.649512
	0.1					0.095964	1.811206
	0.3					0.131032	0.827806
	0.5					0.226795	0.546835
		0.5				0.922375	0.127935
		0.7				0.055464	0.777028
		0.9				0.032777	1.126142
			1.2			0.325552	0.361757
			1.4			0.442143	0.362171
			1.6			0.940627	0.363232
				0.2		0.326196	0.361986
				0.4		0.737809	0.443502
				0.6		0.981247	0.874884
					0.3	0.326113	0.337170
					0.6	0.326115	0.359627
					0.9	0.326119	0.362171

5 Conclusion

5.1 Novelty, Prospectus, and Recommendation

The main objectives of this article are subsequently, we utilize the numerical method bvp4c by MATLAB to solve the governing equations. The governing equations have been converted into an ordinary differential system with suitable conversions. The numerical method Runge-Kutta fourth-order is employed to solve non-linear ordinary differential equations. A set of non-linear ordinary differential equations is obtained in the form of second-order f, θ and ϕ. The simulation study is focused on applying nondimensional parameters. The research results have been transported in the form of a graphical representation. This investigation aims to determine the conclusion of governing parameters on velocity, temperature, concentration, and micro-organisms.

5.2 Importance of work

In modern years, the investigation of bio-convection is a very popular area of research outstanding due to its extensive range of presentations such as cancer treatment, water distillation, manufacturing of aircraft, and medicines, and efficiency of electronic instruments. The main aim of this exploration is to analyze the chemical reaction on the buoyancy-driven flow of thermal radiation with the suspension of micro-organisms; which are all applied to the flow of parabolic and cone of revolution to establish governing equations. The primary outcomes are summarized below.

- Velocity reduces against chemical reaction parameter γ.
- Temperature profile increases for Nb, Nr and decreases for $\gamma \; and \; Pe$.
- Concentration profile increases for γ, Nr, Nb and decreases for Nt, Pe.
- Microorganism profile increases for γ, Pe and decreases for Nt, Nr.
- Influence of radiation parameter on Nusselt number (Nu) has enhanced the Sherwood number (Sh).
- Impact of Brownian parameter on Nusselt number (Nu) has enhanced the opposite done in Sherwood's number (Sh).
- Impact of Peclet parameter on Nusselt number (Nu) and Sherwood number (Nu) has enhanced in both conditions.

References

1) Saleem S, Gopal D, Nehad A, Shah N, Feroz N, Kishan JD, et al. Modelling entropy in magnetized flow of eyring-powell nanofluid through nonlinear stretching surface with chemical reaction: a finite element method approach, . *Nanomaterials*. 2022;12:1811–1811. Available from: https://doi.org/10.3390/nano12111811.
2) Majeed A, Golsanami N, Gong B, Qazi A, Ahmad S, Rifaqat A, et al. Analysis of thermal radiation in magneto-hydrodynamic motile gyrotactic micro-organisms flow comprising tiny nanoparticle towards a nonlinear surface with velocity slip. *Alexandria Engineering journal*. 2023;66:543–553. Available from: https://doi.org/10.1016/j.aej.2022.11.012.
3) Yang Y, Jiang WQ, Wu YH, Wang P, Wu Z, Zhang B, et al. Migration of buoyancy-controlled active particles in a laminar open-channel flow. *Advances in Water Resources*. 2021;156:104023–104023. Available from: https://doi.org/10.1016/j.advwatres.2021.104023.
4) Majeed A, Zeeshan A, Ali S, Noori FM. Consequence of thermophoresis and brownian motion on three-dimensional magnetohydrodynamic casson nanofluid flow with heat transfer analysis. *Transactions of ARazmadze Mathematical Institute*. 2022;176(1). Available from: https://doi.org/10.1166/jon.2019.1687.
5) Kumar YM, Shah NA, Nagendramma V, Durgaprasad P, Sivakumar N, Rao BM, et al. Linear regression of triple diffusive and dual slip flow using Lie Group transformation with and without hydro-magnetic flow. *AIMS MATHEMATICS*. 2023;8(3):5950–5979. Available from: https://doi.org/10.3934/math.2023300.
6) Kumar R, Sood S, Raju C, Shehzad SA. Hydromagnetic unsteady slip stagnation flow of nanofluid with suspension of mixed bio-convection, . *Propulsion and Power Research*. 2019;8:362–372. Available from: https://doi.org/10.1016/j.jppr.2018.10.001.
7) Sangeetha E, De P. Bioconvective Casson nanofluid flow toward stagnation point in non-Darcy porous medium with buoyancy effects, . *chemical reaction, and thermal radiation*. 2023;52:1529–1551. Available from: https://doi.org/10.1002/htj.22753.
8) Sreelakshmi TK, Selvi PD, Babu KR, Prasad PD, Santosh HB, Abraham A, et al. Dynamics of Brownian motion and nonlinear mixed convective conditions on thermophoretic slip flow embedded with non-Fourier flux. *International Journal of Modern Physics B*. 2024;38(10):2450144–2450144. Available from: https://doi.org/10.1142/S0217979224501443.
9) Jagadha S, Naik SHS, Durgaprasad P, Kumar AN, Naikoti K. Radiative Newtonian Carreau nanofluid through stretching cylinder considering the first-order chemical reaction. *International Journal of Ambient Energy*. 2022;43(1):4959–4967. Available from: https://doi.org/10.1080/01430750.2021.1929473.
10) Ellahi R. The effects of MHD and temperature dependent viscosity on the flow of non-Newtonian nanofluid in a pipe: Analytical solutions. *Applied Mathematical Modelling*. 2013;37(3):1451–1467. Available from: https://doi.org/10.1016/j.apm.2012.04.004.
11) Mehboob J, Ellahi R, Sait SM. Analytical Investigation of Thermal Radiation Effects on Electroosmotic Propulsion of Electrically Conducting Ionic Nanofluid with Single-Walled Carbon Nanotube Interaction in Ciliated Channels, . *Symmetry*. 2024;16:717–717. Available from: https://doi.org/10.3390/sym16060717.
12) Zeeshan A, Khalid N, Ellahi R, Khan MI, Sultan Z, Alamri. Analysis of nonlinear complex heat transfer MHD flow of Jeffrey nanofluid over an exponentially stretching sheet via three phase artificial intelligence and Machine Learning techniques. *Solitons & Fractals*. 2024;189:115600–115600. Available from: https://doi.org/10.3390/sym16060717.

13) Zeeshan A, Ellahi R, Rafique MA, Sadiq M, Sait, Shehzad. Parametric Optimization of Entropy Generation in Hybrid Nanofluid in Contracting/Expanding Channel by Means of Analysis of Variance and Response Surface Methodology, . *Inventions*. 2024;9(5):92–92. Available from: https://doi.org/10.3390/inventions9050092-27.
14) Khan AA, Arshad A, Ellahi R, Sait S. Heat transmission in Darcy Forchheimer flow of Sutterby nanofluid containing gyrotactic microorganisms. *International Journal of Numerical Methods for Heat & Fluid Flow*;2023(1):135–152. Available from: https://doi.org/10.1108/HFF-03-2022-0194.
15) Othman A, Ali H, Jubair B, S. Numerical simulation of the nanofluid flow consists of gyrotactic microorganism and subject to activation energy across an inclined stretching cylinder. *Sci Rep*. 2023;13:7719–7719. Available from: https://doi.org/10.1038/s41598-023-34886-2.
16) Ahmed J, Nazir F, Fadhl MB, Makhdoum MB, Mahmoud Z, Mohamed A, et al. Magneto-bioconvection flow of Casson nanofluid configured by a rotating disk in the presence of gyrotatic microorganisms and Joule heating, . *Heliyon*. 2023;9. Available from: https://doi.org/10.1016/j.heliyon.2023.e18028.
17) Abbas M, Khan N, Shehzad SA. Numerical analysis of Marangoni convected dusty second-grade flow in a suspension of chemically reactive microorganisms. *Proceedings of the Institution of Mechanical Engineers*. 2024;238(10):4400–4417. Available from: https://doi.org/10.1177/09544062231209828.
18) Algehyne EA, Areshi M, Saeed A, Bilal M, Kumam W, Kumam P. Numerical simulation of bioconvective Darcy Forchhemier nanofluid flow with energy transition over a permeable vertical plate. *Scientific Reports*. 2022;12(1):3228–3228. Available from: https://dx.doi.org/10.1038/s41598-022-07254-9.
19) Li Y, Majeed A, Ijaz N, Barghout K, Ali MR, Muhammad T. Melting thermal transportation in bioconvection Casson nanofluid flow over a nonlinear surface with motile microorganism: Application in bioprocessing thermal engineering,. *Case Studies in Thermal Engineering*. 2023;49. Available from: https://doi.org/10.1016/j.csite.2023.103285.
20) Sangeetha E, De P. Gyrotactic microorganisms suspended in MHD nanofluid with activation energy and binary chemical reaction over a non-Darcian porous medium. *Waves in Random and Complex Media*. 2022;p. 1–17. Available from: https://doi.org/10.1615/JPorMedia.2020036165.
21) Gopal D, Firdous H, Saleem S, Kishan N. Impact of convective heat transfer and buoyancy on micropolar fluid flow through a porous shrinking sheet: An FEM approach. *Proceedings of the Institution of Mechanical Engineers*. 2022;236:3974–3985. Available from: https://doi.org/10.1177/09544062211045649.
22) Jagadha S, Gopal D, Kumar PV, Kishan N, Durgaprasad P. Three dimensional MHD nanoluid stagnation point low withhigher order chemical reaction. *Journal of Thermal Engineering*. 2022;8(2):286–298. Available from: https://dx.doi.org/10.18186/thermal.1086264.
23) Bhatti MM, Rashidi MM. Effects of thermo-diffusion and thermal radiation on Williamson nanofluid over a porous shrinking/stretching sheet. *Journal of Molecular Liquids*. 2016;221:567–573. Available from: https://dx.doi.org/10.1016/j.molliq.2016.05.049.
24) Mustafa M, Hayat T, Pop I, Asghar S, Obaidat S. Stagnation-point flow of a nanofluid towards a stretching sheet. *International Journal of Heat and Mass Transfer*. 2011;54(25-26):5588–5594. Available from: https://dx.doi.org/10.1016/j.ijheatmasstransfer.2011.07.021.
25) Ibrahim W, Shankar B, Nandeppanavar MM. MHD stagnation point flow and heat transfer due to nanofluid towards a stretching sheet. *International Journal of Heat and Mass Transfer*. 2013;56(1-2):1–9. Available from: https://dx.doi.org/10.1016/j.ijheatmasstransfer.2012.08.034.